Exp. Theo. NANOTECHNOLOGY 6 (2022) 93 - 100 https://doi.org/10.56053/6.3.93

Fabrication of GaN-based LEDs

S-H. Chang[1], *Y. Hou*[2,*]

[1]Department of Physics, Chung Yuan Christian University, Taoyuan 320314, Taiwan, ROC
[2]Institute of Zhejiang University – Quzhou, Quzhou 324000, China
*) Email: houyz@zju.edu.cn

Received 22/2/2022, *Accepted*, 13/9/2022, *Published* 15/10/2022

The authors propose a simple Ar plasma treatment method to selectively damage the area underneath p-pad electrode of GaN-based light-emitting diodes (LEDs). It was found that we could form a highly resistive area so that the injected carriers will be forced to spread out horizontally for the LED. Under 20 mA current injection, it was found that the output powers were 16.0, 17.9 and 17.3 mW while the forward voltages were 3.17, 3.19 and 3.20 V for conventional LED and LED with SiO_2 layer, respectively. Moreover, the LED with Ar plasma treatment is superior to the other LEDs while operating at a higher injection current.

Keywords: GaN; LED; Fabrication.

1. INTRODUCTION

GaN-based light-emitting diodes (LEDs) are important devices that are being used extensively in our daily life. For example, these devices are used in traffic light lamps, outdoor full-color displays and backlight of liquid crystal display panels [1–5]. In order to replace the conventional fluorescent lighting source with solid-state lighting, a great effort for improving the light extraction efficiency is still needed. To approach solid-state lighting, the easiest way to improve output efficiency of GaN-based LEDs is to improve the current spreading due to the insufficient current spreading between p-GaN and transparent conductive layer. Most commercial GaN-based LEDs use an Mg-doped GaN layer as the top p-contact material [6–9]. However, the operation voltage of such LEDs is still high due to the low Mg ionization percentage. The low Mg ionization percentage will result in a highly resistive top p-GaN layer. Thus, current spreading is still an important issue for GaN-based LEDs. Even with the transparent current spreading layer, such as Ni/Au or indium–tin–oxide (ITO), portion of the injected carriers will still be confined underneath the thick metal bonding pad. As a result, a

significant amount of current will be crowded around the p-pad electrode.

To solve this problem, Hu et al. inserted an insulating SiO_2 current blocking layer (CBL) underneath the p-pad electrode [10]. To form this CBL, however, it is necessary to add an extra dry etching step to partially remove the epitaxial layer followed by an extra plasma enhanced chemical vapor deposition (PECVD) step to refill the etched area with SiO_2. Instead of the CBL, Chang et al. simply inserted a PECVD SiO_2 layer between the p-pad and p-GaN to improve current spreading and enhance the light output intensity by 22% [11]. It is also possible to solve this problem by selectively activating the p-GaN layer and form a highly resistive un-activated region underneath the p-pad electrode [12]. Although this method is low cost and easy to implement, one needs to carefully control the activation temperature of the p-GaN layer. The other possible method to form a highly resistive region is to selectively introduce damages underneath the p-contact pad. It has been reported previously that one can use Ar plasma treatment to form highly resistive GaN region by significantly reducing carrier density in the GaN epitaxial layer [13]. Similar to hydrogen treatment, the decrease in carrier density was attributed to the deactivation of dopants by Ar plasma [14]. In this study, we report the use of Ar plasma treatment to selectively damage the area underneath p-pad electrode of GaN-based LEDs. Compared with the deposition of a PECVD SiO_2 layer, it should be noted that introducing Ar plasma treatment should be easier. Optical and electrical properties of the fabricated LEDs will also be discussed.

2. EXPERIMENT

Samples used in this study were all grown by metalor-ganic chemical vapor deposition on 2 in sapphire (0001) substrates. Details of the growth procedures can be found elsewhere [13–15]. The LED structure consists of a 50-nm-thick GaN nucleation layer grown at 550 1C, a 3-mm-thick Si-doped n-GaN buffer layer grown at 1050 1C, an undoped InGaN/GaN multiquantum well (MQW) active region grown at 770 1C, a 50-nm-thick Mg- doped p-$Al_{0.15}Ga_{0.85}N$ electron blocking layer grown at 1050 1C, a 0.6-mm-thick Mg-doped p-GaN layer grown at 1050 1C and a Si-doped $n^þ$ short-period-superlattice (SPS) tunnel contact structure [16–18]. The InGaN/GaN MQW active region consists of five pairs of 3-nm-thick $In_{0.23}Ga_{0.77}N$ well layers and 7-nm-thick GaN barrier layers. The as-grown samples were subsequently annealed at 750 1C in N_2 ambient to activate Mg in the p-type layers.

Using standard photolithography, the samples were then partly etched by an inductively coupled plasma (ICP) etcher until the n-GaN layer was exposed. Standard photolithography was then used again to expose the p-contact region. The samples were subsequently loaded onto a reactive ion etching (RIE) system and treated with Ar plasma for 2 min. During plasma treatment, the flow rate of inlet Ar gas, rf power, bias power and chamber pressure were kept at 100 sccm, 100 W, 100 W and 8 mTorr, respectively. It should be noted that these parameters were optimized. A higher discharge, larger bias powers and/or longer treatment time will all cause severe damage on the sample surface. This consequently will result in degraded device performances. After plasma treatment, an ITO layer was deposited onto the sample surface to serve as the transparent p-contact layer. Furthermore, Ti/Al/Ti/Au was deposited on top of the ITO layer and the exposed n-GaN layer to serve as the p-pad electrode and n-pad electrode, respectively. For comparison, conventional LED and LED with a PECVD SiO_2 layer were also fabricated. Fig. 1(a), (b) and (c) shows schematic diagrams of conventional

LED (i.e., LEDI), LED with Ar plasma treatment (i.e., LEDII) and LED with SiO_2 layer (i.e., LEDIII), respectively. It should be noted that the plasma treated area shown in Fig. 1(b) and the area of SiO_2 layer shown in Fig. 1(c) were both around 100 mm^2.The fabricated epitaxial wafer was then lapped down to about 100 mm and cut into the size of 250 mm x 580 mm chips. These LED chips were then packaged into LED lamps. Current–voltage (*I–V*) measurements of the fabricated LEDs were then performed by an HP2400 semiconductor parameter analyzer. Intensity–current (*L–I*) characteristics were also measured from the top of the devices using molded LEDs with an integrated sphere detector by injecting different amounts of DC current into these LED samples. Circular transmission line model (CTLM) was also used to determine the contact properties between ITO and the LEDs with/without Ar plasmatreatment.

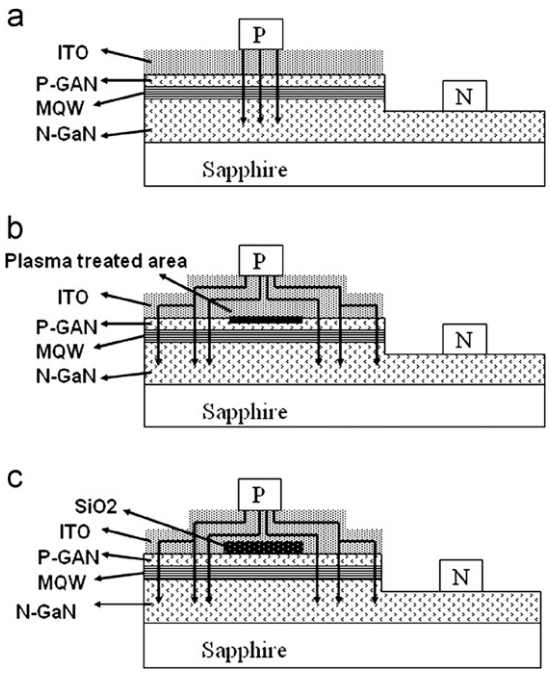

Figure 1 Schematic diagram of (a) conventional LED (i.e., LEDI), (b) LED with Ar plasma treatment (i.e., LEDII) and (c) LED with SiO_2 layer (i.e., LEDIII).

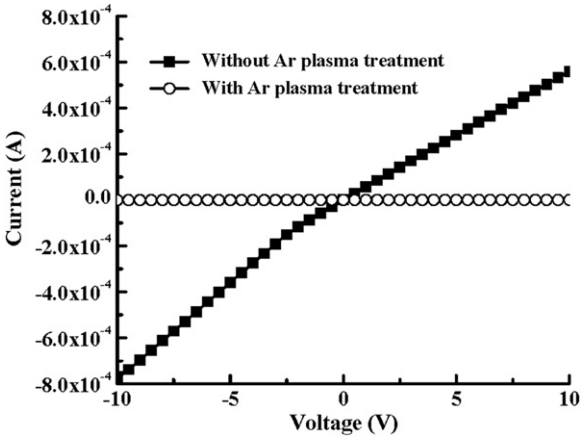

Figure 2 *I–V* characteristics of ITO deposited on LEDs with/without Ar plasma treatment.

3. RESULTS AND DISCUSSION

Fig. 2 shows *I–V* characteristics of ITO deposited on LEDs with/ without Ar plasma treatment. These data were measured with a CTLM spacing of 25 mm. Without Ar plasma treatment, it was found ITO deposited on LED surface shows an ohmic contact property that could be confirmed from the linear curve of *I–V* characteristics (i.e., the $n^þ$-SPS tunnel contact structure) [16]. With Ar plasma treatment, however, it was found that sample surface became insulated and almost no current could be injected into the LED. Such an insulating nature should be attributed to the damages induced by the Ar plasma treatment. As shown in Fig. 1(a), current crowding would occur since most carriers injected from the p-pad electrode will flow vertically downward for conventional LEDs. With the highly resistive layer formed underneath the p-pad electrode, the injected carriers would be forced to spread out horizontally for the LED with Ar plasma treatment, as shown in Fig. 1(b). The enhanced current spreading would also occur for the LED with SiO_2 layer, as shown in Fig. 1(c).

Fig. 3 shows intensity–current–voltage (*L–I–V*) characteristics of the three fabricated LEDs measured at room temperature. It could be seen that the output powers of all these three LEDs increased with the injection current initially, reached a maximum and then started to decrease as the current was further increased. It should be noted that electroluminescence (EL) peak position occurred at 450 nm for all these three LEDs when injected with 20 mA DC current. Under the same injection current, it was found that the largest output power was obtained from LEDII with Ar plasma treatment, followed by LEDIII with SiO_2 layer while output power of the conventional LEDI was the smallest. Under 20 mA current injection, it was found that the output powers were 16.0, 17.9 and 17.3 mW for LEDI, LEDII and LEDIII, respectively. It was also found that the maximum output powers occurred at 120, 150 and 130 mA for LEDI, LEDII and LEDIII, respectively. For the conventional LEDI, a significant amount of heat would be generated and accumulated around the p-pad electrode due to current crowding. As a result, the smallest output power and the earliest occurrence of the maximum output power could be observed. Compared with LEDIII, it should be noted that the output power was larger while the maximum output power occurred later for LEDII. Under high

current injection, the SiO_2 layer inserted underneath the p-pad electrode could result in a large thermal resistance for LEDIII. Thus, LEDII with Ar plasma treatment achieved the largest output power instead of LEDIII with SiO_2 layer. Under 20 mA current injection, it was also found that forward voltages were 3.17, 3.19 and 3.20 V for LEDI, LEDII and LEDIII, respectively. The slightly larger forward voltage observed from the LEDII and LEDIII should be attributed to the reduction of total contact area between the epitaxial layer and the p-pad electrode. It should be noted that the 3.19 V operation voltages observed from LEDII with Ar plasma treatment are still electrically acceptable.

Fig. 4(a) and (b) shows output power mappings for these LEDs
injected with 20 and 100 mA DC current, respectively, measured by a charge-couple-device (CCD) image sensor. It could be seen again that the output power of LEDII was the largest followed by LEDIII while the output power of LEDI was the smallest. As shown in Fig. 4(a) with 20 mA current injection, it was found that light output power distributed more uniformly for LEDII, as compared to LEDI and LEDIII. Such a difference became more apparent as the injection current increased to 100 mA, as shown in Fig. 4(b). It was demonstrated that LEDs with the Ar plasma treated p-GaN surface could perform a better and uniform current spreading result under a higher current injection. This could be attributed to a higher operation current accompanied with a larger saturated current injection.

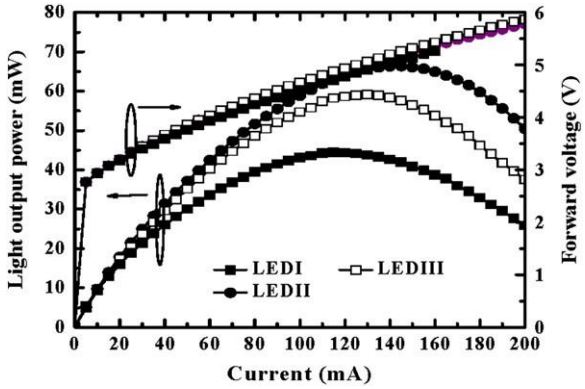

Figure 3 *L–I–V* characteristics of the three fabricated LEDs measured at room temperature.

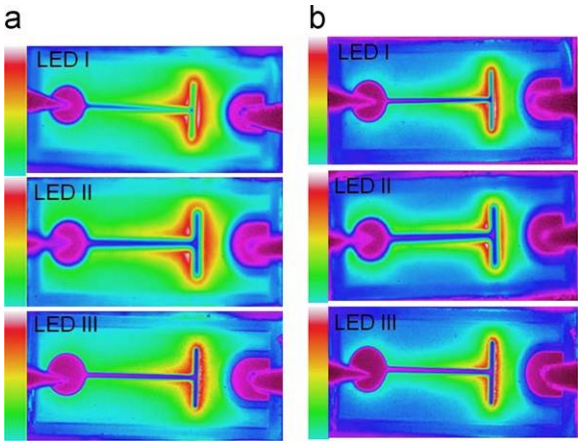

Figure 4 Output power intensity mappings for conventional LED (LEDI), LED with Ar plasma treatment (LEDII) and LED with SiO_2 layer (LEDIII) injected with (a) 20 and (b) 100 mA DC current.

4. CONCLUSION

In summary, we proposed a simple Ar plasma treatment method to selectively damage the area underneath p-pad electrode of GaN-based LEDs. It was found that we could form a highly resistive area so that the injected carriers would be forced to spread out horizontally for the LED. Using the Ar plasma treatment method, it was found that we could effectively increase LED output power while still achieving good forward voltage.

References

[1] Abdulrahman Khaleel Suliman, Mustafa Saeed Omar, Exp. Theo. NANOTECHNOLOGY 5 (2021) 65
[2] Schubert EF, Kim JK. Science 308 (2005) 1274
[3] Omar A. Abdulrazzaq, Siham M. Saeed, Zainab H. Ali, Saad A. Tuma, Omar A. Ahmed, Abdulkareem A. Faridoon, Shaima K. Abdulridha, Exp. Theo. NANOTECHNOLOGY 5 (2021)77
[4] Lan WH. IEEE Transactions on Electron Devices 52 (2005) 1217
[5] Wang WK, Wuu DS, Lin SH, Han P, Horng RH, Hsu TC, et al. IEEE Journal of Selected Topics in Quantum Electronics 41 (2005) 1403
[6] Cuong TV, Cheong HS, Kim HG, Kim HY, Hong CH, Suh EK, Applied Physics Letters 90 (2007) 131107
[7] Sheu JK, Hung IH, Lai WC, Shei SC, Lee ML. Applied Physics Letters 93 (2008) 103507
[8] Kim HG, Cuong,1 TV, Jeong H, Woo SH, Cha OH, Suh EK, Applied Physics Letters 92 (2008) 061118
[9] Lin HC, Lin RS, Chyi JI. Applied Physics Letters 92 (2008) 161113
[10] Huh C, Lee JM, Kim DJ, Park SJ. Journal of Applied Physics 92 (2002) 2248
[11] Chang SJ, Shen CF, Chen WS, Ko TK, Kuo CT, Yu KH, Electrochemical and Solid-State Letters 10 (2007) H175
[12] Liu CC, Chen YH, Houng MP, Wang YH, Su YK, Chen WB, IEEE Photonics Technology Letters 16 (2004) 1444
[13] F. Vervliet, D. Willinger, L. C. Alvarez, Exp. Theo. NANOTECHNOLOGY 5 (2021) 169
[14] Polyakov AY, Smirnov NB, Govorkov AV, Baik KH, Pearton SJ, Luo B, Journal of

Applied Physics 92 (2003) 3960
[15] Chang SJ, Wei SC, Su YK, Chuang RW, Chen SM, Li WL. IEEE Photonics Technology Letters 17 (2005) 1806
[16] Chang SJ, Chang CS, Su YK, Lee CT, Chen WS, Shen CF, et al. IEEE Transactions on Advanced Packaging 28 (2005) 273
[17] Alfarooq O. Basheer, S. Abdullah2, V. K. Arora, Exp. Theo. NANOTECHNOLOGY 5 (2021) 175
[18] A. Subhi, M. A. Saeed, Exp. Theo. NANOTECHNOLOGY 5 (2021) 181
[19] Chang SJ, Chang CS, Su YK, Chuang RW, Lin YC, Shei SC, IEEE Journal of Quantum Electronics 39 (2003) 1439